



Modeling intercontinental transport of ozone in North America with CAMx for the Air Quality Model Evaluation International Initiative (AQMEII) Phase 3

Uarporn Nopmongcol, Zhen Liu, Till Stoeckenius, and Greg Yarwood

Ramboll Environ, 773 San Marin Dr., Suite 2115, Novato, CA 94945, USA

Correspondence to: Uarporn Nopmongcol (unopmongcol@ramboll.com)

Received: 2 March 2017 – Discussion started: 15 March 2017

Revised: 23 June 2017 – Accepted: 3 July 2017 – Published: 24 August 2017

Abstract. Intercontinental ozone (O_3) transport extends the geographic range of O_3 air pollution impacts and makes local air pollution management more difficult. Phase 3 of the Air Quality Modeling Evaluation International Initiative (AQMEII-3) is examining the contribution of intercontinental transport to regional air quality by applying regional-scale atmospheric models jointly with global models. We investigate methods for tracing O_3 from global models within regional models. The CAMx photochemical grid model was used to track contributions from boundary condition (BC) O_3 over a North American modeling domain for calendar year 2010 using a built-in tracer module called RTCMC. RTCMC can track BC contributions using chemically reactive tracers and also using inert tracers in which deposition is the only sink for O_3 . Lack of O_3 destruction chemistry in the inert tracer approach leads to overestimation biases that can exceed 10 ppb. The flexibility of RTCMC also allows tracking O_3 contributions made by groups of vertical BC layers. The largest BC contributions to seasonal average daily maximum 8 h averages (MDA8) of O_3 over the US are found to be from the mid-troposphere (over 40 ppb) with small contributions (a few ppb) from the upper troposphere–lower stratosphere. Contributions from the lower troposphere are shown to not penetrate very far inland. Higher contributions in the western than the eastern US, reaching an average of 57 ppb in Denver for the 30 days with highest MDA8 O_3 in 2010, present a significant challenge to air quality management approaches based solely on local or US-wide emission reductions. The substantial BC contribution to MDA8 O_3 in the Intermountain West means regional models are particularly sensitive to any biases and errors in the BCs. A sensitivity simulation with reduced BC O_3 in response to 20 % lower

emissions in Asia found a near-linear relationship between the BC O_3 changes and surface O_3 changes in the western US in all seasons and across the US in fall and winter. However, the surface O_3 decreases are small: below 1 ppb in spring and below 0.5 ppb in other seasons.

1 Introduction

Intercontinental ozone (O_3) transport extends the geographic range of O_3 air pollution impacts and makes local air pollution management more difficult (Jaffe et al., 2003; Zhang et al., 2011; Emery et al., 2012). The Air Quality Model Evaluation International Initiative (AQMEII) aims to better understand uncertainties in regional-scale model predictions and foster continued model improvement by providing a collaborative, cross-border forum for model development and evaluation in North America and Europe (Galmarini and Rao, 2011). While phases 1 and 2 of the AQMEII focused on performance of different types of regional-scale models, Phase 3 (AQMEII-3) examines the contribution of intercontinental transport to regional air quality by applying regional-scale atmospheric models jointly with global models (Galmarini et al., 2017). Other AQMEII-3 objectives include assessing the sensitivity of regional transport to emissions changes in key source regions worldwide and intercomparing the performance of global and regional-scale models. Multiple models were applied in the AQMEII-3 for North American (NA) and European (EU) regional domains with each model required to track the inflow of O_3 from the lateral domain boundaries at various vertical heights. As in previous phases of AQMEII

the organizers made key model input data available to promote consistent model applications and simplify interpretation of results across participating models.

We applied the Comprehensive Air Quality Model with Extensions (CAMx) photochemical grid model (Ramboll Environ, 2015) for the NA domain using model inputs provided by the AQMEII. Our simulations address the first two objectives of AQMEII-3 by evaluating contributions introduced via boundary conditions (BCs) as inert tracer (i.e., excluding photochemical removal process) and examining O₃ response to reduction of anthropogenic emissions in East Asia or globally. Our study is unique in that we are the only AQMEII-3 participants to also track BC O₃ using chemically reactive tracers.

2 Methodology

2.1 Base case modeling

Air quality modeling for the NA domain and calendar year 2010 used CAMx version 6.2 (Ramboll Environ, 2015) to simulate formation and transport of O₃. Gas-phase chemistry was included using the Carbon Bond (CB05) mechanism (Yarwood et al., 2005), but heterogeneous-phase chemistry was not included for efficiency and because the focus is on O₃. The CAMx modeling domain covers the continental US with 459 by 299 grid cells of 12 km by 12 km resolution and 26 vertical layers (Table S1 in the Supplement). The vertical height of the first layer is 20 m. Model inputs were prepared from data provided to all AQMEII participants supplemented by other data sources (described later). The 2010 annual simulation was initialized on 22 December 2009 to limit the influence of initial concentrations.

This study uses reactive tracers with a chemical mechanism compiler (RTCMC) in CAMx to track contributions from BCs. The RTCMC module simulates explicit tracers in parallel to the host model and represents sources (emissions and BCs), transport processes (advection and diffusion), deposition, and user-defined chemistry (Yarwood et al., 2014). RTCMC chemistry can use species concentrations from the host model, e.g., OH radical, in the reactions of tracers. If no chemistry is defined for an O₃ tracer, then it becomes chemically inert and deposition is the only sink. Currently, the RTCMC models dry deposition of tracers but not wet deposition, which will result in conservative estimates of BC contributions.

CAMx can also track BC O₃ contributions through the ozone source apportionment technology (OSAT; Ramboll Environ, 2015) module, but we use RTRAC because it offers flexibility to model reactive and inert tracers, and to track BC O₃ from specific groups of vertical layers. Vertical attribution is valuable in identifying height ranges of transported O₃ that are most influential to ground-level O₃. Baker et al. (2015) compared RTCMC and OSAT over North

America and found that the two approaches estimated very similar BC O₃ contributions in warmer months. Baker et al. also evaluated computational efficiency of RTCMC tracers. We use the same RTCMC scheme for reactive O₃ tracers as Baker et al. (2015) (Table S2), which includes O₃ destruction by odd hydrogen (i.e., HO₂ and OH) and alkenes but not O₃ destruction by NO because this would entail tracking conversion of BC O₃ to/from several NO_y species, including NO₂, PAN and HNO₃. OSAT accounts for O₃ destruction by NO and Baker et al. show that omission of O₃ destruction by NO in the RTCMC scheme causes some positive bias in BC O₃ estimates in winter months (Baker et al., 2015).

The BC O₃ contributions are analyzed in terms of MDA8 by season because the MDA8 is relevant to the US National Ambient Air Quality Standard (NAAQS) for O₃, which is set at a level of 70 ppb. Seasonal averages are used to evaluate how BC contributions depend upon transport patterns and photochemistry.

2.1.1 Meteorology

Meteorological data for calendar year 2010 were developed by the US Environmental Protection Agency (EPA) for AQMEII phase 2 using the Weather Research Forecast (WRF; Skamarock et al., 2008) model with 12 km resolution. The WRF domain was defined in Lambert conformal projection with 471 by 311 grid cells and 35 vertical layers with a 20 m deep surface layer. The WRF physics options were described in Gilliam et al. (2012). The WRF-CAMx preprocessor reformatted WRF output for CAMx and diagnosed vertical mixing parameters. CAMx employed fewer vertical layers (26) than WRF (35) to reduce the computational burden of the air quality simulations. The CAMx vertical layers exactly matched those used in WRF for the lowest 10 layers (up to 577 m); above this height several WRF layers were combined to single CAMx layers (Table S1). The minimum vertical diffusivity (K_v) was set to 0.1–1.0 m² s⁻¹ based on input landuse.

2.1.2 Emissions

Anthropogenic and fire emissions for 2010 were provided by AQMEII (Pouliot et al., 2015) separately for surface emissions and six elevated source groups, namely fires, international marine shipping, electric generating units (EGU), other point sources (non-EGU), Mexico point sources, and Canada point sources. Biogenic emissions were obtained from the Model of Emissions of Gases and Aerosols from Nature version 2.1 (MEGAN; Guenther et al., 2006; Sakulyanontvittaya et al., 2008). MEGAN has a global database of land cover derived from satellite data at 1 km resolution. Meteorological input data for MEGAN (i.e., temperature and solar radiation) were taken from the WRF predictions. Annual emissions in 2010 in the modeling domain for each source sector are summarized in Table 1.

2.1.3 Boundary conditions

BCs were provided by the European Centre for Medium-Range Weather Forecasts (ECMWF). The ECMWF BC data were based on the Composition-Integrated Forecast System (C-IFS) model (Flemming et al., 2015), which outputs 3-hourly, three-dimensional gridded concentrations which were formatted for CAMx.

We tracked contributions from O₃ BCs in three height ranges defined at the CAMx boundaries, namely from layers 1 to 16 (layers below 750 mb; lower troposphere, LT), 17 to 23 (layers between 750 and 240 mb; middle troposphere, MT), and 24 to 26 (layers above 250 mb; upper troposphere and lower stratosphere, UTLS). We introduced both reactive and inert O₃ tracers for the same vertical groups. Reactive tracers undergo chemical decay according to chemistry scheme defined using the RTCMC, whereas inert tracers only participate in physical processes with no chemical removal. Table S2 presents the RTCMC chemistry scheme for reactive tracers as well as the physical properties for both reactive and inert tracers.

2.2 Sensitivity scenarios

Two sensitivity simulations defined by AQMEII were conducted to quantify O₃ response to anthropogenic emission reductions. The GLO scenario reduced all anthropogenic emissions by 20 % globally and the EAS scenario reduced anthropogenic emissions in the East Asia by 20 %. In the GLO scenario, the CAMx NA anthropogenic emissions were reduced by 20 % for the entire modeling domain with no changes to fire and biogenic emissions. Under the EAS scenario the CAMx NA emissions are the same as in the base case. ECMWF provided BCs specific for each scenario. The ECMWF BCs inadvertently omitted H₂O₂ for the EAS scenario and so we followed the AQMEII suggestion to use H₂O₂ from the base case for both the EAS and GLO scenarios. Other modeling inputs are unchanged from the base case. The annual CAMx sensitivity simulations were conducted with the inert and active boundary O₃ tracers described above. Several metrics are used when comparing sensitivity scenarios to the base case including the fourth highest maximum daily 8 h average (H4MDA8), the average of the 30 highest MDA8 O₃ days (Top 30), and seasonal average MDA8. We show the results for the entire modeling domain and additionally discuss our findings for 22 selected major cities in a wide variety of climatic and geographic environments (Fig. S1 in the Supplement). Cities are represented by the monitoring site with highest H4MDA8 in the metropolitan statistical area.

Table 1. Annual emissions by source sector in 2010 (thousand short tons per year; 1 short ton = 0.907185 metric tons).

Sector	NO _x	VOC	CO
<i>Elevated sources</i>			
EGU (ptipm)	2141	41	691
Non-EGU (ptnonipm)	1558	323	2047
International shipping (c3marine)	1186	45	99
Mexico (mexpt)	384	50	153
Canada (canpt)	504	577	834
Fire (ptfire)	198	1783	13 172
<i>Low-level sources</i>			
Anthropogenic surface	13 067	15 562	58 672
Biogenic	728	53 469	4309
<i>Total</i>	19 765	71 850	79 977

3 Results

3.1 Model performance evaluation (MPE) of ozone

We evaluate O₃ model performance for the base case relative to benchmarks that are accepted in NA. Predictions of MDA8 O₃ are evaluated against observations from the Clean Air Status and Trends Network (CASTNET; rural) and the Air Quality System (AQS; urban and rural). Observations are considered valid when at least 75 % of data are available. A 40 ppb O₃ cutoff is applied to focus on the upper end of O₃ frequency distributions. Statistical metrics used in this evaluation include two bias metrics (normalized mean bias, NMB; fractional bias, FB) and two error metrics (normalized mean error, NME; fractional error, FE) (Table 2). Table 3 shows that model biases (NMB, FB) are less than ±12 % and errors (NME, FE) up to 15 % for all seasons and both networks, well within the bias/error goals of less than ±15 % and 35 % recommended by EPA (1991). The model tends to overestimate O₃ in spring and summer, while it underestimates in fall and winter. Model biases and errors are slightly improved, by less than 2 %, at CASTNET sites. The AQS network includes many urban sites that are heavily impacted by local emissions not well resolved by our modeling grid.

The seasonal spatial distributions of NMB, NME, and Pearson's correlation coefficient (r) at individual CASTNET and AQS sites are shown in Figs. S2–S5. The springtime performance is weakest ($|r| < 0.5$) in the western US, where high terrain prevails. Stratospheric O₃ intrusions are influential in the high terrain of the western US during spring (Langford et al., 2009, 2015; Lin et al., 2012b; Emery et al., 2012) but models do not always represent this process accurately. In summer, the performance is weakest along the Gulf Coast and California coast. Model performance against AQS observations is presented separately for selected 22 major cities. CAMx performs well at these cities, with NMB of −12 to 12 % and NME of 12 to 21 % for MDA8 with zero thresh-

Table 2. Model performance metrics, where $\langle o \rangle$ is the mean and σ_o is the standard deviation of the observed (o) or modeled (m) concentrations (C).

Metric (potential range)	Equation
Normalized mean bias (%) (−100 % to +∞)	$\text{NMB} = \frac{\sum_{i=1}^N (C_m - C_o)}{\sum_{i=1}^N C_o} \quad \text{NME} = \frac{\sum_{i=1}^N C_m - C_o }{\sum_{i=1}^N C_o}$
Normalized mean error (%) (0 % to +∞)	
Fractional bias (%) (−200 to +200 %)	$\text{FE} = \frac{1}{N} \sum_{i=1}^N \frac{ C_m - C_o }{\left(\frac{C_o + C_m}{2}\right)} \quad \text{FB} = \frac{1}{N} \sum_{i=1}^N \frac{(C_m - C_o)}{\left(\frac{C_o + C_m}{2}\right)}$
Fractional error (%) (0 to +200 %)	
Correlation coefficient	$r = \frac{1}{N-1} \sum_{i=1}^N \left(\frac{C_m - \langle C_m \rangle}{\sigma_m} \right) \left(\frac{C_o - \langle C_o \rangle}{\sigma_o} \right)$
Root mean square error	$\text{RMSE} = \sqrt{\frac{\sum_{i=1}^N (C_m - C_o)^2}{N}}$

Table 3. Seasonal and annual model performance statistics for MDA8 O₃ (with 40 ppb cutoff) at AQS and CASTNET sites.

Season	Network	No. obs.	Mean	NMB (%)	NME (%)	FB (%)	FE (%)	<i>r</i>	RMSE
Spring	AQS	71 074	53.6	2.7	10.9	2.6	10.8	0.61	7.44
	CASTNET	5737	54.2	1.9	10.3	1.9	10.2	0.63	7.11
Summer	AQS	72 548	57.3	5.6	13.4	5.4	13.0	0.61	9.53
	CASTNET	5029	56	5.5	12.4	5.6	12.1	0.63	8.47
Fall	AQS	41 729	48.7	−5.9	12.1	−6.4	12.4	0.68	8.26
	CASTNET	3597	47.3	−7.3	10.9	−7.6	11.2	0.71	7.24
Winter	AQS	11 823	40	−10.6	14.0	−11.8	15.1	0.30	8.35
	CASTNET	2328	41.3	−9.0	12.1	−10.0	13.1	0.51	6.67
Annual	AQS	197 174	53.1	1.3	12.3	0.9	12.2	0.64	8.48
	CASTNET	16 691	51.5	−0.4	11.3	−0.7	11.4	0.66	7.52

See Table 2 for definitions of the statistical metrics.

old (Table S3), satisfying the bias/error goals. The performance statistics improve when applying a 40 ppb threshold (Table S4). We additionally provide quantile–quantile (Q–Q) plots (Fig. S8) which compare independently sorted (time-unpaired; space-paired) observed and modeled O₃ for each city. The Q–Q plots suggest good model distributions (e.g., data pairs near the 1 : 1 line) for Los Angeles, Sacramento, Phoenix, Denver, Dallas, Houston, Pittsburgh, and Philadelphia.

We evaluated vertical profiles of O₃ at Trinidad Head (41.0541, −124.151°) on the northern coast of California (Figs. S6 and S7). This location is indicative of O₃ entering the US with prevailing winds from the Pacific Ocean and useful for evaluating O₃ BCs over the Pacific. CAMx reproduces the strong gradient in O₃ starting at the tropopause (between ~ 10 and ~ 14 km) but sometimes underestimates

O₃ near the model top (~ 16 km). In the free troposphere (~ 1 to ~ 10 km), CAMx performance is reasonable with a mix of over- and underpredictions. In the marine boundary layer (MBL; < 500 m), CAMx tends to overpredict surface O₃ because the model lacks a consistently observed gradient toward lower O₃ (typically lower than 50 ppb) at the surface. Potential causes are too little O₃ deposition to the ocean, a lack of O₃ destruction by halogen chemistry in the MBL, too strong vertical mixing in the MBL, or a combination of factors. The influence of low bias in the Pacific MBL will be confined to west coast states because this air is blocked effectively by western mountain ranges (see Sect. 3.5). However, similar biases in the MBL over the Gulf of Mexico and Atlantic Ocean could influence O₃ across the southern and eastern US (see Sect. 3.2). Further analysis is required to address this uncertainty.

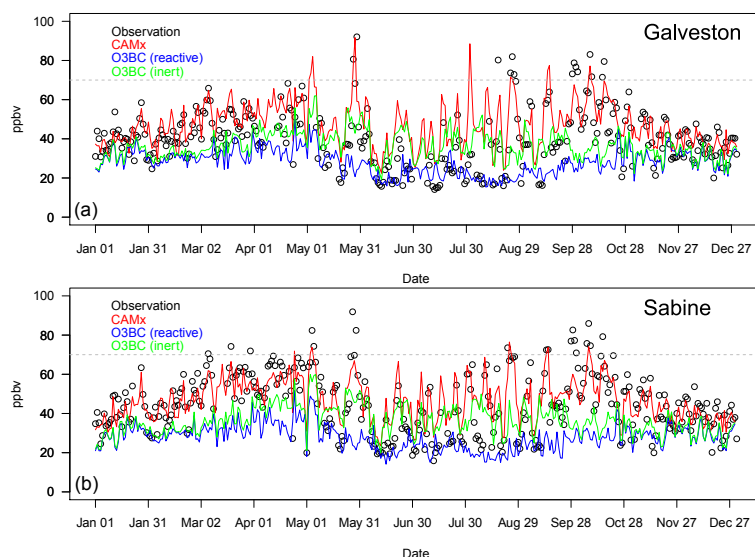


Figure 1. Observed (black circle) and CAMx-predicted (red line) daily MDA8 O₃ at Galveston (**a**; coordinates: 29.254474, -94.861289°), and Sabine Pass (**b**; coordinates: 29.727931, 93.894081°) monitoring sites located on the Texas Gulf Coast near Houston and Beaumont, respectively. Contributions are shown for inert (green line) and reactive (blue line) BC O₃ tracers summed over boundary height ranges.

3.2 Regional MPE analysis at remote sites along the Gulf Coast

We found a consistent high bias for summer O₃ at sites near the Gulf Coast and investigated potential causes using our tracer simulation results. Global modeling studies have reported high-O₃ bias simulated in air arriving along the Texas coast (Fiore et al., 2002, 2014; McDonald-Buller et al., 2011; Zhang et al., 2011). The high-O₃ bias over 10 ppb has been reported by a regional modeling study (Sarwar et al., 2015; Smith et al., 2015). Adding reactions of halogens (especially iodine; Smith et al., 2015) to the O₃ chemistry in CAMx mitigated (e.g., ~ 3 ppb reduction of MDA8 O₃ at coastal sites) but did not eliminate this bias. This study provides an opportunity to examine whether bias in O₃ BCs could contribute to O₃ bias along the Gulf Coast.

Time series of daily MDA8 O₃ together with O₃ BC contributions are shown in Fig. 1 for Galveston and Sabine Pass in Texas. CAMx tends to overpredict O₃ during summer months when onshore winds are prevalent (TCEQ, 2016) due to the enhancement of the Bermuda High bringing warm air from the Gulf of Mexico (Zhu and Liang, 2013). During this period CAMx has a large overprediction bias exceeding 15 ppb at the two sites when observations are low (~ 20 ppb). Reactive O₃ tracers exceed observed O₃ by an average of 2–3 ppb, which explains only a portion of the total model bias, so other factors must be contributing (not examined here). Inert O₃ tracers are on average higher than the reactive tracers by 10–12 ppb, demonstrating that inert tracers can overestimate BC contributions.

3.3 BC ozone contributions to surface ozone

BC contributions based on the active tracers to seasonal average MDA8 O₃ over the US are higher in spring than summer (Fig. 2). Spring contributions are over 40 ppb across the western US, which is the region most influenced by pollution transported from Asia (Jaffe et al., 2003; Zhang et al., 2011; Lin et al., 2012a; Emery et al., 2012). In particular, high-O₃ events over the high terrain in the western US have been linked to intercontinental transport and stratospheric intrusions (Lin et al., 2012a, b). The highest modeled contributions occur in spring, which is consistent with observations (Parish et al., 2012; Cooper et al., 2012) and previous modeling studies (Emery et al., 2012; Fiore et al., 2014). BC contributions in the eastern US are generally below 40 ppb in spring and below 30 ppb in other seasons.

BC contributions on high-O₃ days are compared to the summer average BC contributions in Fig. 3 for 22 major cities. The metrics for high O₃ are the H4MDA8, which is relevant to the NAAQS but is a single day, and the Top 30, which includes a variety of conditions that can lead to high O₃. They are compared to the summer average MDA8 O₃ metric which includes high- and low-O₃ days. In 15 of the 22 major cities (Los Angeles, Sacramento, Dallas, Kansas City, St. Louis, Chicago, Atlanta, Cincinnati, Columbus, Detroit, Pittsburgh, Baltimore, Philadelphia, New York, and Boston), the BC contribution to the Top 30 and summer average days differs by less than 15%, indicating that higher O₃ on the Top 30 days is mainly attributable to larger O₃ production within the modeling domain. BC contributions to the H4MDA8 are smaller than to the Top 30 in 16 of the 22 cities, which is consistent with greater destruction of BC O₃ by lo-

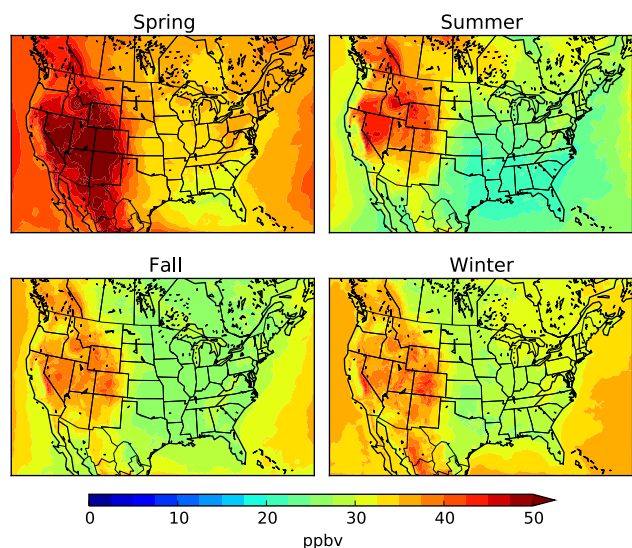


Figure 2. BC contributions to seasonal average MDA8 O₃ from reactive tracers summed over boundary height ranges.

cal photochemistry on the highest O₃ days in these cities. Los Angeles and Sacramento fall in this category with BC contributions to H4MDA8 below 20 ppb. For the cities east of the Rocky Mountains the H4MDA8 contributions range from 19 ppb (St. Louis) to 34 ppb (Detroit) and the differences among the three metrics are generally within 5 ppb with no metric consistently being highest or lowest. In contrast, for cities in the Intermountain West (Boise, Phoenix, Salt Lake, and Denver) the BC contribution is consistently lower for summer average than the two high-O₃ day metrics (i.e., differences are more than 8 ppb). For Denver, our model estimates 57 ppb of BC contribution to the Top 30 and 72 ppb to the H4MDA8. However, the modeled 72 ppb BC contribution to the Denver H4MDA8 is certainly overstated, because the observed MDA8 on this day was only 50 ppb, and we place more emphasis on metrics like the Top 30 that consider multiple days. BC contributions tend to be higher in the western than the eastern US because of higher terrain and deeper planetary boundary layer (PBL) that can efficiently transport mid-tropospheric O₃ to ground level, and longer O₃ lifetimes in the PBL (Fiore et al., 2002).

We further investigated how total O₃ changes as the modeled BC contributions increase (in 10 ppb increments) as shown in Fig. 4 for several cities. The relationships vary between cities and the model captures this variation with the western cities (Denver and Phoenix) showing different patterns than eastern cities (Philadelphia and Atlanta). For Denver and Phoenix in the Intermountain West, total O₃ increases with BC contribution and approaches the 1 : 1 line at higher BC contribution, revealing small groups of days when MDA8 O₃ exceeded 60 ppb (11 days for Denver and 7 days for Phoenix) and the modeling indicates that BCs accounted for almost all of this O₃. In other words, BC contributions alone

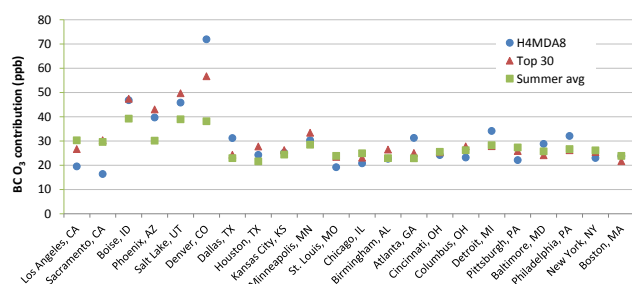


Figure 3. BC O₃ contributions to the H4MDA (blue dot), average MDA8 on the Top 30 MDA8 O₃ days (red triangle), and summer average MDA8 (green square) at 22 major cities.

distinguish high-O₃ days from low days. These groups of high BC-contributed days are important because local emission reductions, or even US-wide emission reductions, would be ineffective at reducing O₃. However, there are other days in Denver when total MDA8 O₃ exceeded 60 ppb with modeled BC contribution below 30 ppb (see first and second bars in Fig. 4) on which reducing local or US emissions would lower O₃. Air quality managers need methods to identify dates when emission reductions would be ineffective so that those dates can be excluded from emission strategy development. Nonetheless, these results should be interpreted with consideration given to model performance. As shown in the Q–Q plot for Denver (Fig. S8), the model can capture the O₃ distribution quite well, although it underestimates MDA8 O₃ over 65 ppb and overestimates MDA8 O₃ over 80 ppb. For this reason, we encourage making use of multi-day metrics (such as Top 30) rather than a single-day metric (e.g., H4MDA8).

3.4 Inert vs. active ozone BCs

Contributions to seasonal average MDA8 from reactive and inert tracers are shown in Fig. 5, where positive differences indicate larger contributions from inert tracers in all seasons. In summer, when photochemistry is active, the differences are more than 10 ppb. At the Galveston and Sabine Pass sites, the differences frequently exceed 20 ppb in summer days (Fig. 1). During spring and fall, contributions from inert tracers are 5 ppb higher than contributions from active tracers in southern regions and less than 5 ppb elsewhere. In winter, when photochemistry is less active, the estimated contributions from the inert and active tracers are similar. Such seasonal variation is consistent across all three groups of vertical layers (Figs. S9–S11). These results emphasize the critical role of O₃ chemistry and highlight the estimation bias inherent to the inert tracer approach.

3.5 O₃ contributions by boundary height range

The largest BC contributions to seasonal average MDA8 O₃ over the US are from the MT with small contributions from

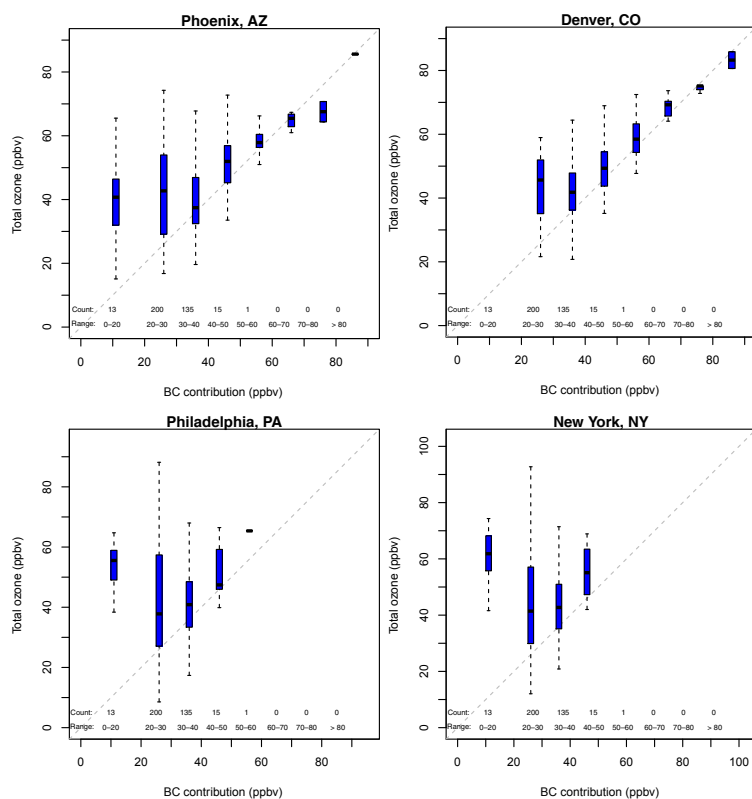


Figure 4. Box-and-whisker plots comparing modeled total MDA8 O_3 to modeled BC contribution in 10 ppb ranges paired in time and space for Phoenix, Denver, Philadelphia, and New York.

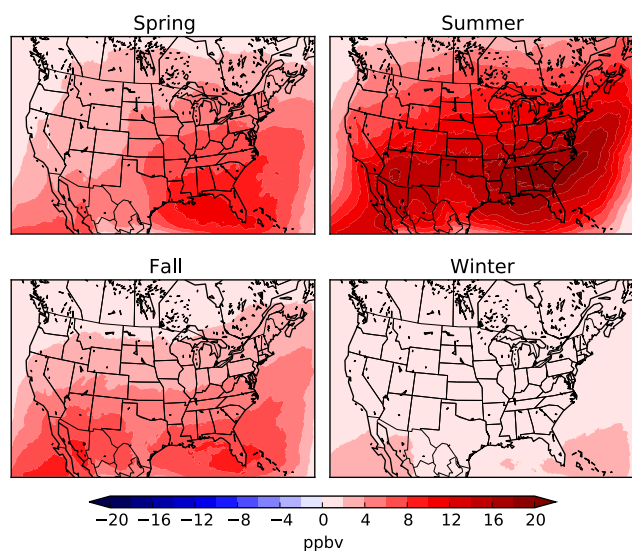


Figure 5. Differences between inert and reactive BC O_3 tracer contributions to seasonally averaged MDA8 O_3 (inert – reactive) summed over all boundary height ranges.

the UTLS (Fig. 6). The contributions from the MT are highest in spring, followed by summer, fall, and winter. The attri-

bution of the MT to spring maxima is over 40 ppb across the western US, but less than 25 ppb in the eastern US. The contributions from the LT are highest (more than 30 ppb) along the western boundary but decrease sharply at the coastline as a result of dilution as the boundary layer moves onshore along with higher O_3 deposition velocities over land. Dissipating contributions from the model boundaries with distance are seen at all lateral sides because O_3 deposits to the earth's surface and is destroyed by chemical reactions in the atmosphere. The penetration of LT BC O_3 inland O_3 peaks in winter, when chemistry and deposition are least active. The UTLS BC tracers contribute only a few ppb, mostly over the highest western terrain, and up to 6 ppb in summer when vertical convection is most active.

3.6 Sensitivity to changing anthropogenic emissions (GLO and EAS scenarios)

Reducing emissions in East Asia by 20 % (EAS scenario) decreases average O_3 across the US in all seasons (Fig. 7, first-column panels). As expected, decreases are highest in the west because the western US is closest to Asia and has high terrain. The O_3 decreases are small: below 1 ppb in spring and below 0.5 ppb in other seasons. Decreases in O_3 BC reactive tracers (Fig. 7, second-column panels) are almost iden-

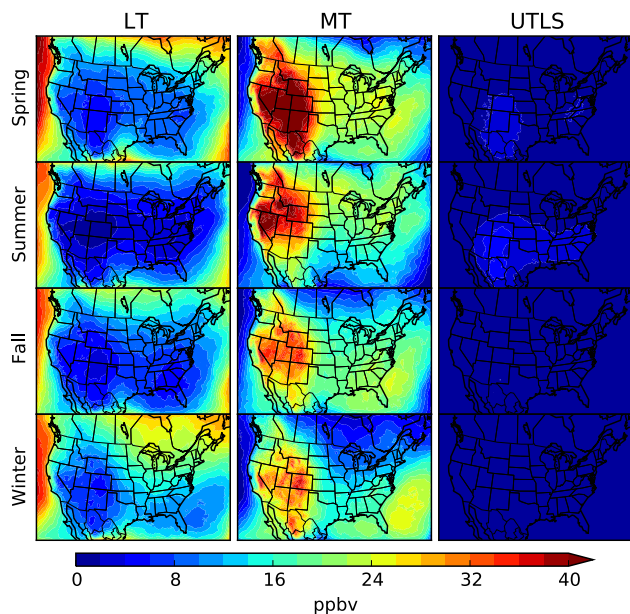


Figure 6. Seasonal average MDA8 O₃ contributions from boundary height ranges using reactive BC O₃ tracers.

tical to modeled O₃ decreases but slightly smaller (e.g., generally within 0.1 ppb) because the reactive tracers omit some chemical interactions.

We examine more closely the relationship between changes in O₃ and reactive tracers in the EAS scenario. In each surface grid cell, we regress hourly O₃ changes against reactive tracer concentration changes (summed over boundary height ranges) to compute slope and r as demonstrated in the two scatter plots for Denver in spring and summer. Slope and r values of 1 indicate that the O₃ changes are explained entirely by the changes in O₃ BC reactive tracers. The delta total O₃ and delta tracer O₃ relationship is near-linear at Denver with a slope of 0.87 and r of 0.9. The 16 panels in Fig. 7 show the regression parameters for each grid surface cell and match the scatter plots for Denver. The slope and r (Fig. 7, third- and fourth-column panels) values have similar spatial patterns in all seasons. In winter and fall the slope values are near 1 with r of 0.8 to 1 across the US, suggesting strong influence of O₃ transport from Asia during these seasons. In spring, strong correlation ($r = 0.8$ to 1) is seen in the western US, but areas in the eastern US have a slope lower than 0.2 and r lower than 0.4, indicating that the O₃ BC tracers can explain only a fraction of the total O₃ change. The lowest correlation ($r < 0.2$) is in the summertime over the southeastern US in a region where the EAS scenario produces almost no change in surface O₃, indicating that transport from Asia becomes unimportant. High correlation in the western US in all seasons emphasizes the influence of O₃ transport from Asia in this region.

Reducing global emissions by 20 % (GLO scenario), including US emissions, decreases summertime average O₃ by

up to 4 ppb (Fig. 8). The largest reductions occur over the eastern US, where US emissions cause domestic O₃ production. O₃ reductions in fall and winter are small, generally lower than 1–2 ppb. Many NO_x-rich areas (e.g., urban cores) show O₃ increases as a result of NO_x emission reductions (i.e., NO_x disbenefit) in all seasons. The spatial pattern and magnitude of the changes in BC O₃ tracers differs from the changes in surface O₃ (Fig. 8, first- and second-column panels) except near the boundaries and in winter. The correlation between changes in surface O₃ and BC tracers is low ($|r| < 0.4$) in all seasons except winter (Fig. 8, fourth-column panels). Overall, in the GLO scenario US surface O₃ is more sensitive to domestic emission reductions than changes in BCs.

We use summer average MDA O₃ to show how the two emission scenarios change BC contributions for the 22 major cities (Fig. 9). The EAS scenario reduces BC contribution in all cities with reductions range from 0.06 ppb (Houston) to 0.3 ppb (Boise). Reductions are larger in the western US and more northern latitude in the eastern US (e.g., larger reduction in Columbus than Atlanta). These reductions result mostly from smaller MT and LT BC contributions because the EAS scenario scaled back the contribution of each height range about equally. The EAS scenario changed the UTLS BC contributions by less than 0.01 ppb. The GLO scenario produced larger reductions than the EAS scenario and they range from 0.4 ppb (Boston) to 1.2 ppb (Los Angeles). These reductions are mainly driven by the MT BCs in all of the cities except Dallas and Houston. Higher influence from the LT in the GLO scenario than the EAS scenario for most cities is consistent with the GLO scenario reducing emissions just outside the CAMx domain, whereas in the EAS scenario the emission reductions occur only in East Asia.

3.7 Comparing BC O₃ contributions in two regional models

The AQMEII activity permits comparison of BC O₃ contributions in different regional models. US EPA applied the CMAQ model over the NA domain with the same model input data as we used with CAMx except for biogenic emissions. The WRF-CMAQ system was configured using WRFv3.4 and CMAQv5.0.2 (Appel et al., 2013; see also Foley et al., 2010, and Byun and Schere, 2006). Options in CMAQ include wet deposition as described in Byun and Schere (2006) and dry deposition as described in Pleim and Ran (2011). Additional details on the CMAQ configuration used in these simulations can be found in Solazzo et al. (2017). Figure 10 compares BC O₃ contributions to seasonal average MDA8 O₃ estimated by CAMx and CMAQ using inert BC O₃ tracers (CMAQ was not run with reactive tracers). Differences between the CMAQ and CAMx inert tracer impacts are smaller than the differences between inert and reactive tracers in CAMx, which exceed 10 ppb (Fig. 5), but they are notable, in a range of 4–8 ppb in sum-

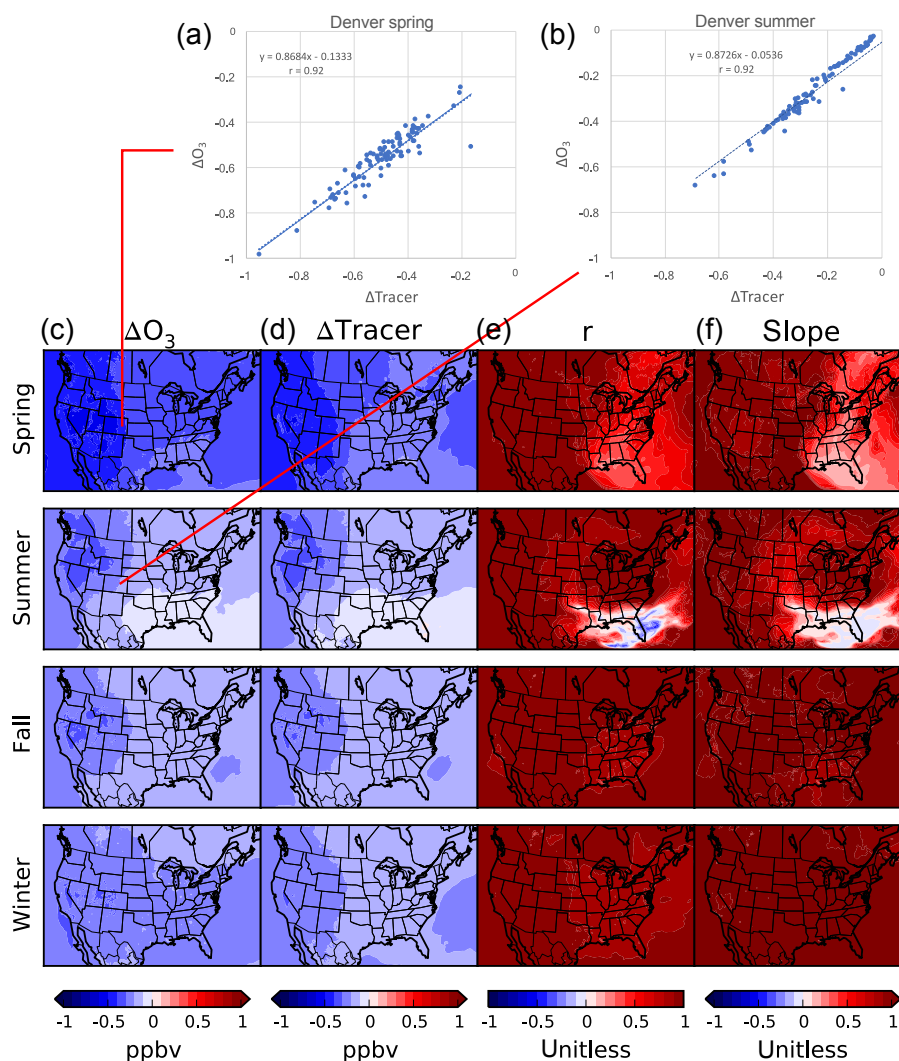


Figure 7. Scatter plots on the top show delta daily average O_3 (y axis) and reactive tracer BC O_3 contribution (x axis) for Denver in spring and summer for 20% reduction in East Asia emissions (EAS scenario). The 16 panels summarize the same information showing seasonal delta total O_3 (c) and reactive tracer BC O_3 contribution (d) for each grid surface. The correlation (r) and slope of a linear regression of (d) against column are shown in columns (e) and (f), respectively.

mer and 2–6 ppb in spring with CAMx being higher. Factors contributing to these differences may include fewer vertical layers in CAMx (26, compared to 35 in CMAQ), allowing greater transport of UTLS O_3 to ground level (Emery et al., 2012), omission of wet scavenging for the CAMx inert tracers, treatment of deep convective transport in CMAQ, or differences in model treatments of O_3 dry deposition. Liu et al. (2017) performed multi-model process comparisons with four AQMEII models and draw similar conclusions regarding factors that can contribute to differences in tracer impacts.

4 Conclusions

The overall MDA8 O_3 performance is within evaluation goals. We do not see evidence of systematic problems with

the model setup, although performance at individual monitor does vary, and the potential for hidden biases and errors always exists. Future studies could benefit from refining model assumptions that may be important at specific sites. For example, overstated MBL O_3 at Trinidad Head is partly attributable to the lack of O_3 destruction by oceanic halogen chemistry. Other possible reasons include insufficient O_3 deposition to the ocean, too strong vertical mixing in the MBL, or a combination of factors. The model tendency to overestimate O_3 in spring may suggest overstated BC contributions as seen at the Denver site. Perfecting model performance at individual sites across the US is not pursued in the current study. If accuracy in estimating BC contributions is critical, such as in demonstrating attainment of O_3 standards, model

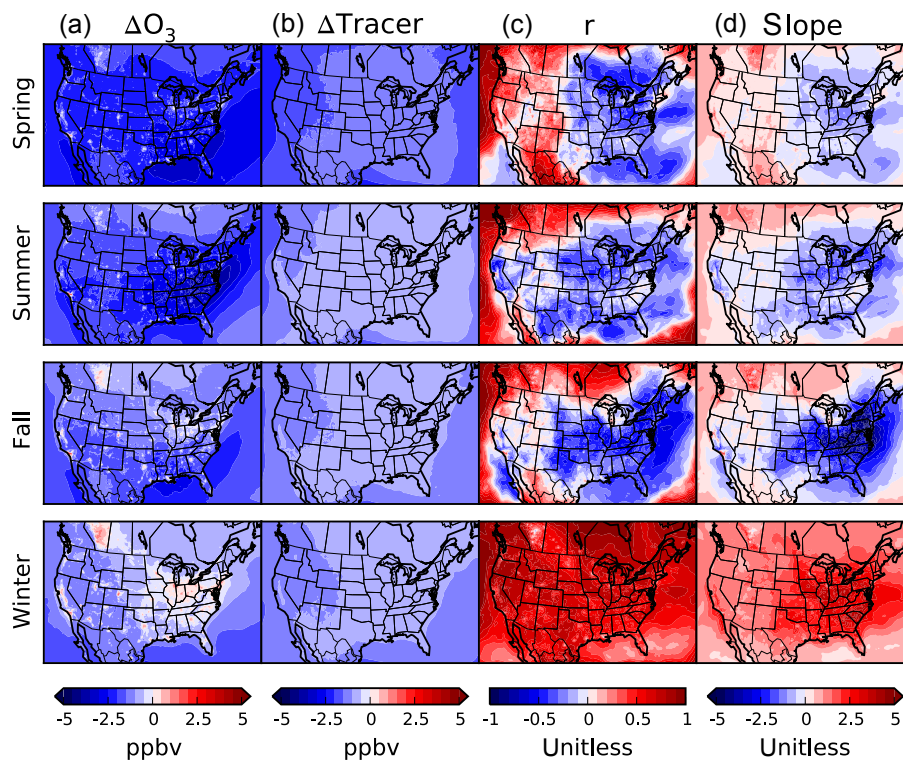


Figure 8. Changes to seasonal average O_3 (a) and reactive tracer $BC\ O_3$ contribution (b) for 20% reduction of global emissions (GLO scenario). The correlation (r) and slope of a linear regression of (b) against column are shown in (c) and (d), respectively.

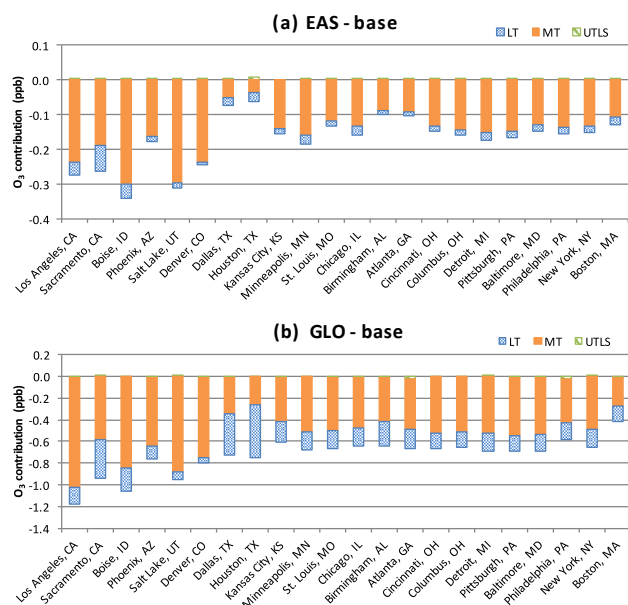


Figure 9. Changes in BC contribution (ppb) to summer average $MDA8\ O_3$ by height range for the EAS (a) and GLO (b) scenarios from the base case.

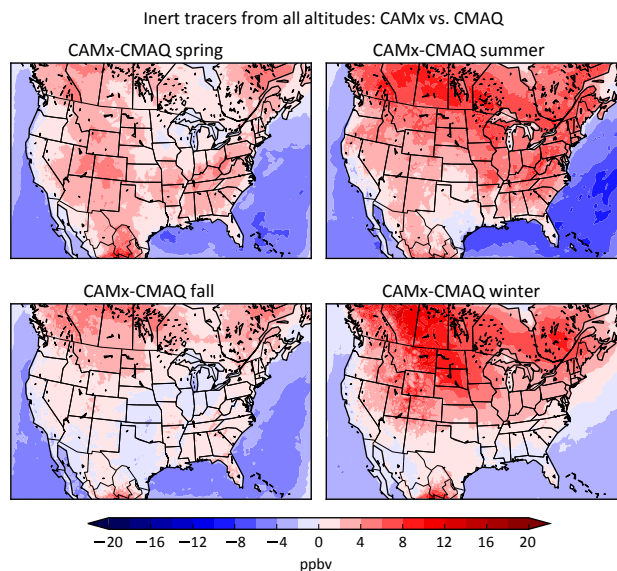


Figure 10. Differences in seasonally averaged $MDA8$ contributions from inert $BC\ O_3$ tracers in CAMx and CMAQ (CAMx-CMAQ).

performance and BC contributions cannot be overlooked, especially on high-O₃ days.

Inert BC O₃ tracers consistently estimate higher BC contributions to seasonal average MDA8 O₃ across the US than reactive tracers, particularly in summer. The inherent bias in the inert tracer approach (i.e., omitting chemical destruction) can exceed 10 ppb in seasonally averaged MDA8 O₃, which is substantial in comparison to the 70 ppb level of the O₃ NAAQS. This information is critical for interpreting results obtained with inert tracers in AQMEII-3 and other studies.

Comparing inert tracers in two regional models that used substantially the same input data found differences in MDA8 O₃ that were generally within 5 ppb, smaller than the differences between inert and reactive tracers run in a single model (CAMx), but nevertheless those inert model differences were notable. Potential causes include differing numbers of model vertical layers (influencing movement of UTLS O₃ to ground level) and differences in model treatments of deposition. This exercise emphasizes that source contribution analyses of BC O₃ (or other non-inert pollutants) using the inert tracer approach should only be interpreted qualitatively, especially during the spring and summer period. Making tracers reactive is a simple improvement that is very important to this type of analysis. Future studies should consider adopting the reactive tracer approach.

Contributions from O₃ BCs in three height ranges (LT, MT and UTLS) differ spatially and temporally. The LT BC tracers do not penetrate very far inland, with contributions to MDA8 O₃ up to 20 ppb in coastal states. The largest contributions to MDA are from the MT BCs with springtime maxima exceeding 40 ppb in the high terrain of the western US. The high contribution of BC O₃ to ground level O₃ in portions of the western US presents a significant challenge to air quality management approaches based solely on local emission reductions. Nonetheless, model comparison with observations suggests that estimated high BC contributions in the Intermountain West could be overstated and that the bias inherited in O₃ BCs can affect model performance. Replicating the highest end of observed O₃ distribution is particularly challenging. We encourage making use of multi-day metrics (such as Top 30) as an alternative to a single-day metric (e.g., H4MDA8) when examining contributions from international transport.

Reducing emissions in East Asia (EAS scenario) revealed a near-linear relationship between changes in BC O₃ and changes in surface O₃ in the western US in all seasons and across the US in fall and winter with a near 1 : 1 slope. However, the surface O₃ decreases are small: below 1 ppb in spring and below 0.5 ppb in other seasons. These reductions result mostly from smaller MT and LT BC contributions because the EAS scenario scaled back the contribution from each height range about equally. In the GLO scenario US surface O₃ is more sensitive to domestic emission reductions than changes in the BCs. Our 2010 EAS contribution results are slightly higher than the estimates of 0.35–0.45 ppb from

a multi-model experiment that also simulated the EAS scenario but for the year 2001 (Reidmiller et al., 2009). This is expected as East Asia emissions have increased over the last decade. Assuming a linear relationship, our study suggests an EAS total contribution of 2.5 ppb in certain seasons based on 0.5 ppb O₃ reduction with 20 % emission decrease. It is difficult to quantify how the model biases affect the O₃ response to emission perturbations because the sources of biases are unknown.

Data availability. CAMx, the model used in the study, can be downloaded from <http://www.camx.com/>. The observed data used to evaluate model performance can be obtained from <https://www.epa.gov/aqs> (AQS) and <https://www.epa.gov/castnet> (CASTNET). The AQMEII modeling inputs used in the study are available to the AQME project participants at the AQME website: <http://aqmeii.jrc.ec.europa.eu/>.

The Supplement related to this article is available online at <https://doi.org/10.5194/acp-17-9931-2017-supplement>.

Competing interests. The authors declare that they have no conflict of interest.

Special issue statement. This article is part of the special issue “Global and regional assessment of intercontinental transport of air pollution: results from HTAP, AQMEII and MICS”. It is not associated with a conference.

Acknowledgements. This study was supported by the Coordinating Research Council Atmospheric Impacts Committee.

We gratefully acknowledge the contribution of various groups to the third air Quality Model Evaluation international Initiative (AQMEII) modeling database used in this work: US EPA, Environment Canada, Mexican Secretariat of the Environment and Natural Resources (Secretaría de Medio Ambiente y Recursos Naturales-SEMARNAT) and National Institute of Ecology (Instituto Nacional de Ecología-INE) (North American national emissions inventories), US EPA (North American emissions processing and meteorology inputs), ECMWF/MACC project, and Météo-France/CNRM-GAME (Chemical boundary conditions). We thank Christian Hogrefe for discussions and CMAQ results.

Edited by: Frank Dentener

Reviewed by: two anonymous referees

References

Appel, K. W., Pouliot, G. A., Simon, H., Sarwar, G., Pye, H. O. T., Napelenok, S. L., Akhtar, F., and Roselle, S. J.: Evaluation of

- dust and trace metal estimates from the Community Multiscale Air Quality (CMAQ) model version 5.0, *Geosci. Model. Dev.*, 6, 883–899, <https://doi.org/10.5194/gmd-6-883-2013>, 2013.
- Baker, K. R., Emery, C., Dolwick, P., and Yarwood, G.: Photochemical grid model estimates of lateral boundary contributions to ozone and particulate matter across the continental United States, *Atmos. Environ.*, 123, 49–62, 2015.
- Byun, D. W. and Schere, K. L.: Review of the governing equations, computational algorithms, and other components of the Models – 3 Community Multiscale Air Quality (CMAQ) Modeling System, *Appl. Mech. Rev.*, 59, 51–77, 2006.
- Cooper, O. R., Gao, R.-S., Tarasick, D., Leblanc, T., and Sweeney, C.: Long-term ozone trends at rural ozone monitoring sites across the United States, 1990–2010, *J. Geophys. Res.*, 117, D22307, <https://doi.org/10.1029/2012JD018261>, 2012.
- Emery, C., Jung, J., Downey, N., Johnson, J., Jimenez, J., Yarwood, G., and Morris, R.: Regional and global modeling estimates of policy relevant background ozone over the United States, *Atmos. Environ.*, 47, 206–217, <https://doi.org/10.1016/j.atmosenv.2011.11.012>, 2012.
- EPA – Environmental Protection Agency: Guidance for Regulatory Application of the Urban Airshed Model (UAM), Office of Air Quality Planning and Standards, Research Triangle Park, NC, 1991.
- Fiore, A. M., Jacob, D. J., Bey, I., Yantosca, R. M., Field, B. D., and Fusco, A. C.: Background ozone over the United States in summer: origin, trend, and contribution to pollution episodes, *J. Geophys. Res.*, 107, 4275, <https://doi.org/10.1029/2001JD000982>, 2002.
- Fiore, A. M., Oberman, J. T., Lin, M. Y., Zhang, L., Clifton, O. E., Jacob, D. J., Naik, V., Horowitz, L. W., Pinto, J. P., and Milly, G. P.: Estimating North American background ozone in U.S. surface air with two independent global models: Variability, uncertainties, and recommendations, *Atmos. Environ.*, 96, 284–300, <https://doi.org/10.1016/j.atmosenv.2014.07.045>, 2014.
- Flemming, J., Huijnen, V., Arteta, J., Bechtold, P., Beljaars, A., Blechschmidt, A.-M., Diamantakis, M., Engelen, R. J., Gaudel, A., Inness, A., Jones, L., Josse, B., Katragkou, E., Marecal, V., Peuch, V.-H., Richter, A., Schultz, M. G., Stein, O., and Tsikerdekis, A.: Tropospheric chemistry in the Integrated Forecasting System of ECMWF, *Geosci. Model. Dev.*, 8, 975–1003, <https://doi.org/10.5194/gmd-8-975-2015>, 2015.
- Foley, K. M., Roselle, S. J., Appel, K. W., Bhave, P. V., Pleim, J. E., Otte, T. L., Mathur, R., Sarwar, G., Young, J. O., Gilliam, R. C., Nolte, C. G., Kelly, J. T., Gilliland, A. B., and Bash, J. O.: Incremental testing of the Community Multiscale Air Quality (CMAQ) modeling system version 4.7, *Geosci. Model. Dev.*, 3, 205–226, <https://doi.org/10.5194/gmd-3-205-2010>, 2010.
- Galmarini, S. and Rao, S. T.: The AQMEII two-continent Regional Air Quality Model Evaluation study: fueling ideas with unprecedented data, *Atmos. Environ.*, 45, 2464, <https://doi.org/10.1016/j.atmosenv.2011.03.025>, 2011.
- Galmarini, S., Koffi, B., Solazzo, E., Keating, T., Hogrefe, C., Schulz, M., Benedictow, A., Griesfeller, J. J., Janssens-Maenhout, G., Carmichael, G., Fu, J., and Dentener, F.: Technical note: Coordination and harmonization of the multi-scale, multi-model activities HTAP2, AQMEII3, and MICS-Asia3: simulations, emission inventories, boundary conditions, and model output formats, *Atmos. Chem. Phys.*, 17, 1543–1555, <https://doi.org/10.5194/acp-17-1543-2017>, 2017.
- Gilliam, R. C., Godowitch, J. M., and Rao, S. T.: Improving the horizontal transport in the lower troposphere with four dimensional data assimilation, *Atmos. Environ.*, 53, 186–201, <https://doi.org/10.1016/j.atmosenv.2011.10.064>, 2012.
- Guenther, A., Karl, T., Harley, P., Wiedinmyer, C., Palmer, P. I., and Geron, C.: Estimates of global terrestrial isoprene emissions using MEGAN (Model of Emissions of Gases and Aerosols from Nature), *Atmos. Chem. Phys.*, 6, 3181–3210, <https://doi.org/10.5194/acp-6-3181-2006>, 2006.
- Jaffe, D., McKendry, I., Anderson, T., and Price, H.: Six ‘new’ episodes of trans-Pacific transport of air pollutants, *Atmos. Environ.*, 37, 391–404, 2003.
- Langford, A. O., Aikin, K. C., Eubank, C. S., and Williams, E. J.: Stratospheric contribution to high surface ozone in Colorado during springtime, *Geophys. Res. Lett.*, 36, L12801, <https://doi.org/10.1029/2009GL038367>, 2009.
- Langford, A. O., Senff, C. J., Alvarez, R. J., Brioude, J., Cooper, O. R., Holloway, J. S., Lin, M. Y., Marchbanks, R. D., Pierce, R. B., Sandberg, S. P., and Weickmann, A. M.: An Overview of the 2013 Las Vegas Ozone Study (LVOS): Impact of stratospheric intrusions and long-range transport on surface air quality, *Atmos. Environ.*, 109, 305–322, 2015.
- Lin, M., Fiore, A. M., Horowitz, L. W., Cooper, O. R., Naik, V., Holloway, J., Johnson, B. J., Middlebrook, A. M., Oltmans, S. J., Pollack, I. B., and Ryerson, T. B.: Transport of Asian ozone pollution into surface air over the western United States in spring, *J. Geophys. Res.-Atmos.*, 117, D00V07, <https://doi.org/10.1029/2011JD016961>, 2012a.
- Lin, M., Fiore, A. M., Cooper, O. R., Horowitz, L. W., Langford, A. O., Levy, H., Johnson, B. J., Naik, V., Oltmans, S. J., and Senff, C. J.: Springtime high surface ozone events over the western United States: Quantifying the role of stratospheric intrusions, *J. Geophys. Res.-Atmos.*, 117, D00V22, <https://doi.org/10.1029/2012JD018151>, 2012b.
- Liu, P., Hogrefe, C., Bieser, J., Im, U., Mathur, R., Nopmongcol, U., Roselle, S., and Spero, T.: Multi-Model Comparison of Lateral Boundary Contributions to Surface Ozone Over the United States, *Atmos. Chem. Phys.* in preparation, 2017.
- McDonald-Buller, E. C., Allen, D. T., Brown, N., Jacob, D. J., Jaffe, D., Kolb, C. E., Lefohn, A. S., Oltmans, S., Parrish, D. D., Yarwood, G., and Zhang, L.: Establishing policy relevant background (PRB) ozone concentrations in the United States, *Environ. Sci. Technol.*, 45, 9484–9497, 2011.
- Parrish, D. D., Law, K. S., Staehelin, J., Derwent, R., Cooper, O. R., Tanimoto, H., Volz-Thomas, A., Gilge, S., Scheel, H.-E., Steinbacher, M., and Chan, E.: Long-term changes in lower tropospheric baseline ozone concentrations at northern mid-latitudes, *Atmos. Chem. Phys.*, 12, 11485–11504, <https://doi.org/10.5194/acp-12-11485-2012>, 2012.
- Pleim, J. and Ran, L.: Surface Flux Modeling for Air Quality Applications, *Atmosphere*, 2, 271–302, 2011.
- Pouliot, G., Denier van der Gon, H., Kuenen, J., Makar, P., Moran, M., and Zhang, J.: Analysis of the Emission Inventories and Model-Ready Emission Datasets of Europe and North America for Phase 2 of the AQMEII Project, *Atmos. Environ.*, 115, 345–360, <https://doi.org/10.1016/j.atmosenv.2014.10.061>, 2015.

- Ramboll Environ: CAMx Users Guide, available at: http://www.camx.com/files/camxusersguide_v6-20.pdf, last access: 5 April 2015.
- Reidmiller, D. R., Fiore, A. M., Jaffe, D. A., Bergmann, D., Cuvelier, C., Dentener, F. J., Duncan, B. N., Folberth, G., Gauss, M., Gong, S., Hess, P., Jonson, J. E., Keating, T., Lupu, A., Marmer, E., Park, R., Schultz, M. G., Shindell, D. T., Szopa, S., Vivanco, M. G., Wild, O., and Zuber, A.: The influence of foreign vs. North American emissions on surface ozone in the US, *Atmos. Chem. Phys.*, 9, 5027–5042, <https://doi.org/10.5194/acp-9-5027-2009>, 2009.
- Sakulyanontvittaya, T., Duhl, T., Wiedinmyer, C., Helmig, D., Matsunaga, S., Potosnak, M., Milford, J., and Guenther, A.: Monoterpene and Sesquiterpene Emission Estimates for the United States, *Environ. Sci. Technol.*, 42, 1623–1629, 2008.
- Sarwar, G., Gantt, B., Schwede, D., Foley, K., Mathur, R., and Saiz-Lopez, A.: Impact of enhanced ozone deposition and halogen chemistry on tropospheric ozone over the Northern Hemisphere, *Environ. Sci. Technol.*, 49, 9203–9211, 2015.
- Skamarock, W. C., Klemp, J. B., Dudhia, J., Gill, D. O., Barker, D. M., Duda, M. G., Huang, X.-Y., Wang, W., and Powers, J. G.: A Description of the Advanced Research WRF Version 3, NCAR Technical Note, NCAR/TN-45+STR, NCAR, Boulder, Colorado, USA, 2008.
- Smith, J. H., Estes, M., Mellberg, J., Nopmongcol, U., and Yarwood, G.: Addressing model over-prediction of ozone influx from the Gulf of Mexico, Presented at Community Modeling and Analysis System (CMAS) conference, available at: <https://www.cmascenter.org/conference/2015/agenda.cfm> (last access: 10 January 2016), 2015.
- Solazzo, E., Bianconi, R., Hogrefe, C., Curci, G., Alyuz, U., Balzarini, A., Baro, R., Bellasio, R., Bieser, J., Brandt, J., Christensen, J. H., Colette, A., Francis, X., Fraser, A., Garcia Vivanco, M., Jiménez-Guerrero, P., Im, U., Manders, A., Nopmongcol, U., Kitwiroon, N., Pirovano, G., Pozzoli, L., Prank, M., Sokhi, R.S., Tuccella, P., Yarwood, G., and Galmarini, S.: Evaluation and Error Apportionment of an Ensemble of Atmospheric Chemistry Transport Modeling Systems: Multi-Variable Temporal and Spatial Breakdown, *Atmos. Chem. Phys.*, 17, 3001–3054, <https://doi.org/10.5194/acp-17-3001-2017>, 2017.
- TCEQ – Texas Commission of Environmental Quality: Illustrations of wind direction movement at particular Texas cities from 1984 to 1992, available at: <https://www.tceq.texas.gov/airquality/monops/windroses.html> (last access: 18 August 2017), 2016.
- Yarwood, G., Rao, S., Yocke, M., and Whitten, G.: Updates to the Carbon Bond Chemical mechanism: CB05, report, Rpt. RT-0400675, US EPA, Res. Tri. Park, 2005.
- Yarwood, G., Emery, C., Baker, K., and Dolwick, P.: Resolving and Quantifying Ozone Contributions from Boundary Conditions Within Regional Models, in: *Air Pollution Modeling and its Application XXIII*, Springer International Publishing, 445–450, https://doi.org/10.1007/978-3-319-04379-1_73, 2014.
- Zhang, L., Jacob, D. J., Downey, N. V., Wood, D. A., Blewitt, D., Carouge, C. C., van Donkelaar, A., Jones, D. B. A., Murray, L. T., and Wang, Y.: Improved estimate of the policy-relevant background ozone in the United States using the GEOS-Chem global model with $1/2 \times 2/3$ horizontal resolution over North America, *Atmos. Environ.*, 45, 6769–6776, <https://doi.org/10.1016/j.atmosenv.2011.07.054>, 2011.
- Zhu, J. and Liang, X.: Impacts of the Bermuda High on Regional Climate and Ozone over the United States, *J. Climate*, 26, 1018–1032, <https://doi.org/10.1175/JCLI-D-12-00168.1>, 2013.